“Ab-initio” synthesis of zeolites for preestablished catalytic reactions

Eva María Gallego,[+] M. Teresa Portilla,[+] Cecilia Paris, Alejandro León-Escamilla, Manuel Moliner, Avelino Corma*

Instituto de Tecnología Química, Universitat Politècnica de València-Consejo Superior de Investigaciones Científicas, Avenida de los Naranjos s/n, 46022 Valencia, España

*Corresponding author: E-mail address: acorma@itq.upv.es

[+] These authors have contributed equally

Abstract (100-150 words):

A new concept and methodology that allows synthesizing active and selective zeolites for preestablished catalytic reactions is presented. It consists of preparing organic structure directing agents that mimic the transition state (TS) of preestablished reactions to be catalyzed. Then, zeolites that maximize the host–guest interaction between the mimic of the transition state and the zeolite framework could be synthesized. In these zeolites, the pores and cavities could be generated approaching a molecular recognition pattern. Two scenarios for synthesizing such “imprinted zeolites” have been considered: a) the TS is larger than the reaction product, and b) the product and the TS have similar size. The concept has been shown to work and zeolite catalysts have been obtained in this way for relevant reactions in the fields of petrochemistry and chemicals.

One Sentence Summary (150 characters):

The use of OSDAs that mimic reaction transition states allows the synthesis of zeolite catalysts with a better molecular recognition adapted for relevant chemical processes.

Zeolites are among the most successful type of materials used in the fields of gas adsorption and separation, and as catalysts for oil conversion, petrochemistry, preparation of chemicals and fine chemicals, as well as for NOx abatement in movil sources (*1-5*). The typical strategy in the field relies on synthesizing new structures and modifying existing ones, and then identifying the most adequate for a particular application in catalysis or adsorption. In other words, there is an important component of trial and error in the existing methodology for synthesis of zeolites and their applicability. Despite the limitations, scientists have achieved a high degree of systematization, and there is a large body of acquired knowledge that helps to approach zeolite synthesis and reactivity (*6, 7*). There is no doubt that development of new methodologies and synthesis concepts that would direct towards the "a priori" design and synthesis of a zeolite for catalyzing a pre-established reaction, could open new perspectives in the field. We have attempted that, starting from the following general principles:

a) A successful solid catalyst for a given reaction should minimize the energy ($AG^{\#}$) of the transition state (TS) of the reaction.
b) An efficient catalyst accelerates reaction through steric and electronic complementarity to reactants during formation of the TS. Thus, a tight binding of the catalyst to the TS, lowers the activation energy, boosting the catalytic activity.
c) The zeolite structure formed in presence of a particular Organic Structure Directing Agent (OSDA) should maximize host-guest interactions, and minimize the energy of the zeolite–organic system.

Taking the above into consideration, we propose to start the synthesis of zeolites by first defining the reaction to be catalyzed. Then, a potential reaction transition state (TS) is stablished, followed by the synthesis of an OSDA that close mimics the TS. If this could be done, such an OSDA could direct toward the synthesis of zeolite structures with

channels and cavities that maximize the host–guest interactions between the OSDA and the zeolite framework. Because the OSDA is very close in shape and charge to the TS of the reaction to be catalyzed, the resulting zeolite should lower the activation energy barrier. In other words, the resultant zeolite, either if already exists or is a new structure, should be suitable to catalyze the desired reaction.

The methodology described above is connected with the field of "imprinted transition state analogues". More precisely, amorphous silica has been used for imprinting mimics of transition states (*8, 9*). However, the difficulties associated with imprinted amorphous silica are derived from the heterogeneity of the sites, as well as from the "mobility" of the gels upon calcinations that may disturb the imprinted shapes and terminal groups (*10*). Superior results had been obtained by attaching in a controlled way functional organic groups to the pores of bulk amorphous silicas (*11, 12*). Then, the imprinting method, while conceptually interesting, shows limitations when amorphous oxides had been applied, due to site accessibility and the lack of stability of the imprinted active voids upon calcination and reaction-regeneration.

The advantage with the synthesis of "imprinted" zeolites concept presented here would be the presence of permanent crystalline structures. Therefore, unmodified cavities with the appropriate shapes and interactions for transition state stabilization will remain after removal of the OSDA by calcination.

In the present work, we have contemplated two possible scenarios for synthesizing "imprinted zeolites". In the first one, the TS is larger than the reaction product, then the reaction product could diffuse freely through the pores of the zeolite. In the second scenario, the product has a similar size than the TS, then, the product diffusion will be limiting. To consider this, we would be synthesizing bidimensional zeolites or

nanocrystalline zeolites where the reaction products formed in the discontinued cavities and channels at the external surface could diffuse out.

We will show in this manuscript that the concept indeed works and, following this, we have found zeolites that maximize selectivity for various relevant catalytic processes in the fields of petrochemicals and chemicals.

RESULTS AND DISCUSSION

1. Reactions involving a TS larger than the reaction product

1.1. Toluene disproportionation

The production of xylenes by toluene disproportionation is a reaction of industrial importance that it is today carried out commercially using mainly ZSM-5 and mordenite zeolites based catalysts (*13*). The disproportionation of toluene involves two molecules of toluene to give one molecule of benzene and one of dimethylbenzene (*o*-, *m*-, *p*-xylenes). As shown in Figure 1A, the postulated transition state (*14*) has a larger molecular size than either of the products formed, i.e., benzene and xylenes. Then, in principle, an OSDA that mimics such a transition state could, in principle, generate zeolites with cavities that would maximize host–guest interactions with such TS. Moreover, it will be large enough to allow diffusion of the reaction products (unless a small pore structure is formed). If so, and looking to the reported TS molecular structure (*14, 15*) with the formal positive charge in the connecting methyl group, different potential TS mimics have been proposed as OSDAs (see Figure 1B).

For the OSDA selection, we consider that an important parameter is also the location of the positive charge within the molecule since this will also fix the position of the active acid site in the structure. For the design of the transition state mimics (TSM) as OSDA we have considered, as it is usually done, not only quaternary ammonium groups but also have introduced the corresponding phosphonium ions. That has a dual purpose; on the

one hand, the phosphonium ions are more stable towards Hoffman degradation than quaternary ammonium ions allowing to explore wider ranges of temperature and pH in the synthesis. On the other hand, we believe that the phosphonium cations will be placed closer to the zeolite framework than the quaternary ammonium, being this in line with the interaction of the carbocation with the T^{III}– $O^{\delta-}$–T^{IV} sites in the reaction transition state.

- *Zeolite synthesis and characterization*

The mimics from Figure 1B have been studied as OSDA for the synthesis of zeolites under the reaction conditions presented in the phase diagrams summarized in Figure S1. The results obtained show that under the present synthesis conditions, only one zeolite crystallizes when the phosphonium mimic TSM_2 (see Figure S1) was used as template. The sample was identified as ITQ–27 (see PXRD pattern in Figure S2A),(*16*) with a crystalline structure composed by a bidirectional pore system of interconnected 12x12-ring openings (see Figure S3). The zeolite has been obtained with a Si/Al ratio of 29 (see Table S1), and crystals are formed as platelets of 1-2 μm (see Figure S4).

In principle, and as per the stated hypothesis concept, this zeolite should be adequate for carrying out the disproportionation of toluene into xylenes. To verify that, we have compared the catalytic behavior of the newly synthesized zeolite with the two zeolites industrially used for carrying out disproportionation of toluene, which, as a note, have been optimized along the years, i.e., ZSM-5 and mordenite. In order to perform a fair comparison, we selected ZSM-5 and mordenite zeolite samples with the same, or close, Si/Al ratios than ITQ-27 (see Experimental). For comparison, we also introduced a sample of Beta zeolite, where the pore topology (12x12x12-rings) will be closer, but not the same than the ITQ-27 obtained here (12x12-rings), which could also easily accommodate the reaction transition state for the disproportionation reaction. The characterization of the zeolite samples, i.e., crystal size and shape, ^{27}Al MAS NMR and

physico-chemical properties are given in Figures S4 and S5, and Tables S1 and S2, respectively.

Following the patent literature on zeolite catalysts for toluene disproportionation (*17, 18*), we have introduced Ni to the zeolites (see experimental) and their characteristics are also given in Tables S1 and S2. The characterization results indicate that all the samples considered have a high micropore volume, and crystallite sites that go from ~1 to 2 µm, except for the mordenite that presents smaller crystallites (0.2 µm) (see Table S1). Most of the Al in the zeolite samples are in tetrahedral coordination (see Figure S5) and, despite the similar Si/Al ratios, mordenite, and ZSM-5, have a larger amount of Brønsted acid sites than ITQ-27, as measured by pyridine adsorption–desorption (see Table S2).

- *Catalytic results*

The Ni-containing samples were tested for toluene disproportionation in a fixed bed continuous reactor at 450°C and 30 bar with a H_2/Toluene molar ration of 4/1. Conversions and selectivities were measured at different contact times (m/F) ranging from 0.1 to 1.1 g. h. mol^{-1} (see experimental). The results, presented in Figure 2A, show that despite its lower concentration of acid sites, the most active zeolite is the one obtained with the mimic of the reaction, i.e., ITQ–27. Its activity is nevertheless very close to mordenite, despite the much larger number of acid sites present in the latter.

In fact, if the turnover frequencies (TOF) per Brønsted acid site (as measured by pyridine) are calculated from initial reaction rates (see Figure 2B), it can be concluded that the order of activity is ITQ-27 > Mordenite ~ Beta > ZSM-5. Moreover, from the selectivity point of view, ITQ-27 appears to give the same or even some higher selectivity to xylenes (see Figure S6).

In conclusion, with a transition state mimic of the toluene disproportionation reaction, a zeolite has been synthesized (ITQ-27) that is intrinsically very active, even surpassing in

activity per active site those industrially zeolites used today, and with high selectivity to xylenes.

1.2. Reaction involving ring expansion and contraction: isomerization of ethylbenzene to xylenes

ZSM-5 and modified ZSM-5 are industrially used to perform the hydroisomerization of xylenes to maximize the *para* isomer. However, the C8 alkylaromatic feed introduced in the process, also contains ethylbenzene (EB), which accumulates during the process and should be either dealkylated or isomerized into xylenes. Isomerization is a more carbon effective process than dealkylation, and zeolite catalysts, and more specifically mordenite, has been used as commercial catalyst for isomerization of EB into xylenes (*19, 20*).

It has been proposed that the mechanism of EB isomerization can go through a partial ring hydrogenation, followed by protonation-ring-expansion-deprotonation and ring contraction (see Figure 3A) (*21*). Thus, taking into account the general hypothesis outlined before, we have attempted to mimic the transition state for ethylbenzene isomerization into xylenes by preparing a seven member ring cationic molecule that could be used as OSDA for the zeolite synthesis (see Figure 3B).

- *Zeolite synthesis and characterization*

The organic molecule shown in Figure 3B that mimics the TS for EB isomerization to xylenes, has been studied as OSDA for the synthesis of zeolites under different experimental conditions. Results in Figure S8 show that only amorphous materials were obtained at lower synthesis temperatures (T=135ºC). Meanwhile, at higher temperatures (150ºC and 175ºC) a new layered aluminosilicate, named LM1, has been obtained together with nanosil. The PXRD pattern (see Figure S9) indicates that LM1 can be a

member of the family of layered silicates that form FER upon calcination, i.e., similar to Prefer (*22*) and PLS-3 (*23*). As a note, there are many other layered silicates that feature the pentasil FER-like layers, i.e. ERS-12 (*24*), MCM-47 (*25*), MCM-56 (*26*), PLS-1 and PLS-4 (*23*), UZM-13 (*27*), etc. However, all of them have been shown to transform upon heating into CDO-type zeolite. Therefore, this later subfamily of layered silicates should more properly be referred as precursors of CDO, or pre-CDO materials.

The PXRD patterns of LM1 and LM1 after calcination (CLM1) resemble those of Prefer and FER materials (see Figure S9). The PXRD patterns of LM1 and CLM1 have been indexed for orthorhombic cells with the following cell dimensions: a=13.992(3) Å, b=7.455(2) Å, and c= 22.847(8) Å and, a=14.106(1) Å, b=7.4530(5) Å, and c= 18.780(1) Å, respectively (see Table S3). Taking the FER structure as reference (see CLM1 in Table S3), there is a 4.07 Å increment in the c axis in LM1 that implies ~2.03 Å between pentasil layers (considering that the radius of oxygen is ~1.35 Å). It is therefore envisioned that the structure of LM1 is held together by hydrogen-bond interactions of silanols from neighboring layers, $\equiv Si_L–O(H)::(H)O–Si_L\equiv$ (Si_L refers to silicon atoms in the pentasil layers, see Figure S10). Comparison of the ^{13}C-CPMAS-NMR spectrum of the as-prepared LM1 and the ^{13}C-NMR of the OSDA indicates that the organic molecule entrapped remains stable during the synthesis (see Figure S12).

From the point of view of catalytic performance, it is very important that the final pore of the zeolite to remain very similar to the expanded pore of the LM1 synthesized with the structure directing agent. Because of that, we cannot simply calcine the sample to produce the 3-D zeolite, since then a contraction will occur and the pore formed could hardly accommodate the transition state of the reaction. Instead, to avoid the contraction of the LM1 into FER, we can perform a simple pillaring by introducing one Si to bridge the layers (see Figure S10). Such a “self-pillaring” can be done by acid treatment of LM1

(*28*), as described in the experimental. By doing that a new zeolite structure, named ITQ-64, with a pore topology formed by 12x10 rings was obtained (see Figure S10). A close examination of the PXRD pattern of ITQ-64 indicates that it should be a more ordered variation of APZ-4 (*28*) and one variation of IEZ-FER (*29*). Then, with the assumption that the structure of ITQ-64 is nearly that of APZ-4, we have calculated the cell dimensions *a*= 14.032(1) Å, *b*= 7.4120(6) and *c*=23.744(2) Å (see Table S3). With respect to LM1, the cell of ITQ-64 is 0.9 Å larger on the *c* axis, normal to the stacking plane. Such an expansion refers to the substitution at z=0 and ½ of the contact $\equiv Si_L–O(H)::(H)O–Si_L\equiv$ in LM1 for the new linkage unit ($\equiv Si_L–O–Si(OH)_2–Si_L$) in ITQ-64. In fact the micropore volume of ITQ-64 is 0.14 $cc.g^{-1}$, which is slightly larger than the calcined LM1 (see Table S4).

The ITQ-64 material presents a Si/Al ratio close to 50 (see Table S4), indicating that the Si/Al ratio remains fairly constant after the pillaring acid treatment and, very interestingly, these Al species are retained in the zeolite framework (see ^{27}Al MAS NMR spectrum of ITQ-64 in Figure S13).

- *Catalytic results*

A commercial catalyst for EB isomerization is a bifunctional Pt/mordenite catalyst that can catalyze the different reaction steps shown in Figure 3A *(20)*. Indeed, the hydrogenating metal function will partially hydrogenate the aromatic ring, which after protonation on the acid sites will form the expanded C7 protonated ring *(30)*. Taking this into account, we have compared the ITQ-64 with two mordenite catalysts containing different Si/Al molar ratios (22 and 47, see MOR_25 and MOR_47, respectively in Table S4), being all these zeolites combined with 1%wtPt/Al_2O_3 in order to introduce the required hydrogenating function to the catalysts (see catalyst preparation in experimental).

When testing these zeolites at the same contact time (~ 5 g.h/mol), it is observed that the high-silica mordenites present higher ethylbenzene conversion values compared to the ITQ-64 zeolite (see Table 1). The higher Brønsted acidities of the mordenite materials, as measured by pyridine (see Table S5), could explain their higher catalytic activities. However, if the turnover frequencies (TOF) per Brønsted acid site are calculated from initial reaction rates, it can be clearly seen that the ITQ-64 shows the highest catalytic activity (see Figure S14). However, the most important observation is that ITQ-64 shows significant higher xylene selectivities compared to the mordenites (see Table 1), even when the zeolites are compared at similar level of conversion (~30%, see Table 1). In fact, if the aromatic selectivity to xylenes obtained with the ITQ-64 is compared with those reported in the literature for many mordenite-based catalysts, it can be seen that ITQ-64 shows higher aromatic selectivty to xylenes than the reported mordenites (see Figure S15).

From the different xylene isomers, the most desired isomers are *p*-xylene, which is used as precursor of polyester (more than 60% of total xylene consumption), and the *o*-xylene, which is used to produce polyester and plasticizers (around 14% of total xylene consumption). Then, it would be very interesting to improve the selectivity towards these isomers. The ITQ-64 material provides higher overall selectivity towards *p*- and *o*-xylenes than the high-silica mordenite zeolites, substantially diminishing the selectivity toward the less desired *m*-xylene (see Figure 4 and Table S6).

In conclusion, following the TSM methodology, it has been possible to synthesize the ITQ-64 zeolite, which is a very promising catalyst for EB isomerization.

2. Reaction involving a TS with similar size that the reaction product: isomerization of adamantane

Adamantane and its derivatives are important tricyclic saturated hydrocarbons for the fields of pharmaceuticals and polymers *(31)*. Adamantane can be found in petroleum mixtures, but its content is very low (less than 0.0004%) (*32*). The most efficient route to prepare adamantane is through *endo*-dicyclopentadiene, which can be easily achieved from a simple Diels-Alder reaction (see Figure S16) *(33-35)*. This process is used at industrial scale using aluminum chloride as isomerization catalyst (see Figure S17).

To avoid the environmental problems associated to the use of aluminum chloride as catalyst, the application of environmentally solid acid as isomerization catalysts would be highly desired. Few reports can be found in the literature studying the use of zeolites for the adamantane synthesis, being zeolite Y the preferred catalyst *(36-38)*.

When the mechanism of the adamantane synthesis has been studied, it has been proposed that the isomerization of the EXO to ADA is the rate controlling step and it occurs through the carbocationic species given in Figure 5A (*39*). If so, it can be observed that the intermediate of the rearrangement reaction presents a similar conformation, including shape and size, that the adamantane product (see Figure 5A). This would mean that the design of a particular zeolite presenting an specfic cavity to allocate the intermediate could, in principle, be made by means of an OSDAwith the adamantane structure, such as N,N,N-trimethyladamantammonium (see TSM_5 in Figure 5B). This is interesting because this organic molecule has been extensively used as OSDA for the synthesis of zeolites, directing to crystallization of the silicoaluminate SSZ-13 zeolite (CHA structure) (*40*). This zeolite is a cage-based material delimited by small pores (3.5 Å), which will not allow the diffusion of the reactants and products involved in the reaction. Besides CHA, TSM_5 has also allowed the synthesis of the ITQ-1 material, which is the high-silica form of the MWW material *(41)*. Unfortunately, the use of the TSM_5, as the only

OSDA, preferentially directs the crystallization of the pure silica ITQ-1 material, precluding its application as acid catalyst.

The crystalline structure of the MWW material is formed by two independent channels with 10-ring pore openings (~5.5 Å), and containing a supercage of 7.1×7.1×18.2 Å (see Figure S17a). This supercage, which is stabilized by the TSM_5 molecule, allows envisioning that the cage-based MWW-type material would permit maximizing the host-guest interactions with the TS of the adamantane isomerization reaction. However, the presence of the medium pores would present severe diffusion restrictions to the molecules involved in the tricyclodecane isomerization. Nonetheless, the cage accessibility may be remarkably improved by preparing the zeolite in 2D form (see Figure S17b) to reduce diffusion limitations of the reactant and products.(*42*)

- *Zeolite synthesis and characterization*

For the particular case of the MWW-related materials, it has been recently described the direct synthesis of the 2-D form of the MWW. This was achieved by using bifunctional OSDAs, presenting a cationic head that allows the crystallization of the MWW layers, and a long aliphatic chain that avoid the layers to grow and order along the *c* axis *(43, 44)*. More specifically, MIT-1 material has been synthesized with an OSDA containing TSM_5 as the cationic head, which can be considered as the TS mimic of the tricyclodecane isomerization (see TSM_6 in Figure 5B). Then, MIT-1 has been synthesized and the adamanatne isomerizartion activiy for adamantane production has been tested. The results are compared with the corresponding 3D MCM-22 (MWW) material and other commercially available large pore zeolites (Beta and USY) with similar Si/Al (see experimental).

The PXRD pattern of the MCM-22 material shows better crystallinity than that of the MIT-1 material (see Figure S18), as it could be expected by its larger order along the *c*

axis (see Figure S17a). Consequently, MIT-1 presents larger external surface area formed by "open" cups than MCM-22 (see Table S7).

- *Catalytic results*

Beta and USY zeolites show high *endo*-tricyclodecane conversion values, but their selectivity toward adamantane is very low for both materials (~5 and 11%, respectively, see Table 2). Their high catalytic activity could be attributed to the presence of large pores in these materials, providing better diffusion pathways to the decane isomers. Similar results have been described for these materials in the literature (*38*) (see Table 2).

In contrast, the two MWW-related materials show a remarkable increase in the selectivity toward the desired adamantane product (above 30%), which is higher than the selectivity observed for the other commercial zeolites (below 11%, see Table 2). This observation could be explained by the adequate fit between the TS of the tricyclodecane isomerization reaction within the MWW-cavity. Indeed, the MIT-1 catalyst, synthesized with a bifunctional TSM of the tricyclodecane isomerization reaction with the aim of favoring not only the formation of MWW cavities but also their accessibility, shows a significant increase of the catalytic activity compared to MCM-22 while maintaining the high adamantane selectivity (~33%, see Table 2).

These results demonstrate the benefits of designing bidimensional zeolites through the transition state mimicking approach when the TS and the desired reaction product show similar sizes.

Conclusions

The new zeolite synthesis methodology based on the design of transition state mimics of relevant industrial reactions to be used as OSDAs for the synthesis of target zeolites has allowed improving the catalytic activity and selectivity of different chemical and petrochemical processes compared to other commercial zeolitic catalysts. In general, the

concept presented here can provide new opportunities for designing more selective adsorption and catalytic solids, as well as sensors and molecular responsive solids.

Acknowledgments

This work has been supported by the European Union through ERC-AdG-2014-671093 (SynCatMatch), and the Spanish Government through "Severo Ochoa Program" (SEV 2012-0267). The Electron Microscopy Service of the UPV is acknowledged for their help in sample characterization. E.M.G. acknowledges "La Caixa - Severo Ochoa" International PhD Fellowships (call 2015). We thank Isabel Millet for technical assistance, and Vicent J. Margarit and Dr. Ángel Cantín for helpful discussions.

Figure 1: (A) Reaction mechanism for the acid catalyzed toluene disproportionation reaction, and (B) Proposed toluene transalkylation transition state mimics (TSM) as organic structure directing agents (OSDAs)

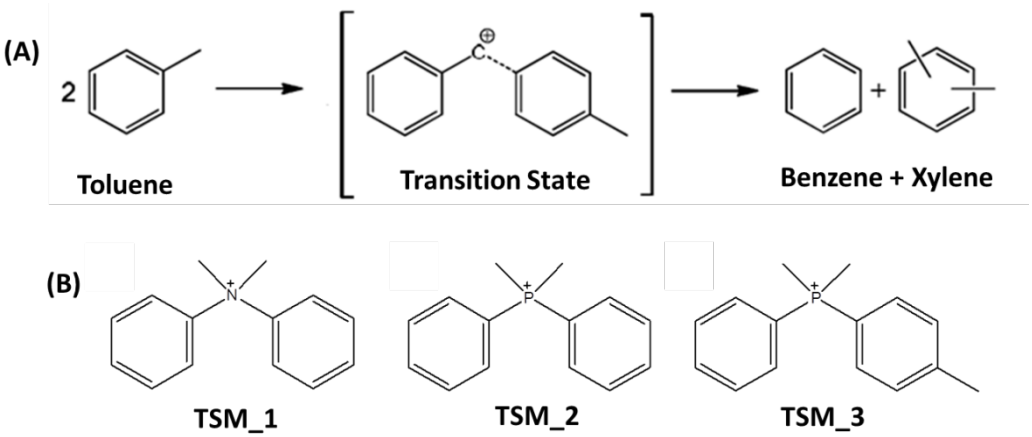

Figure 2: (A) Toluene conversion obtained for the toluene disproportionation reaction in vapor phase at 450ºC and 30 bar with 30 s of time-on-stream (TOS) under different contact times (m/F = 0.1-1.1 g.h/mol); (B) TOF normalized per measured acid site (B423) at different WHSV

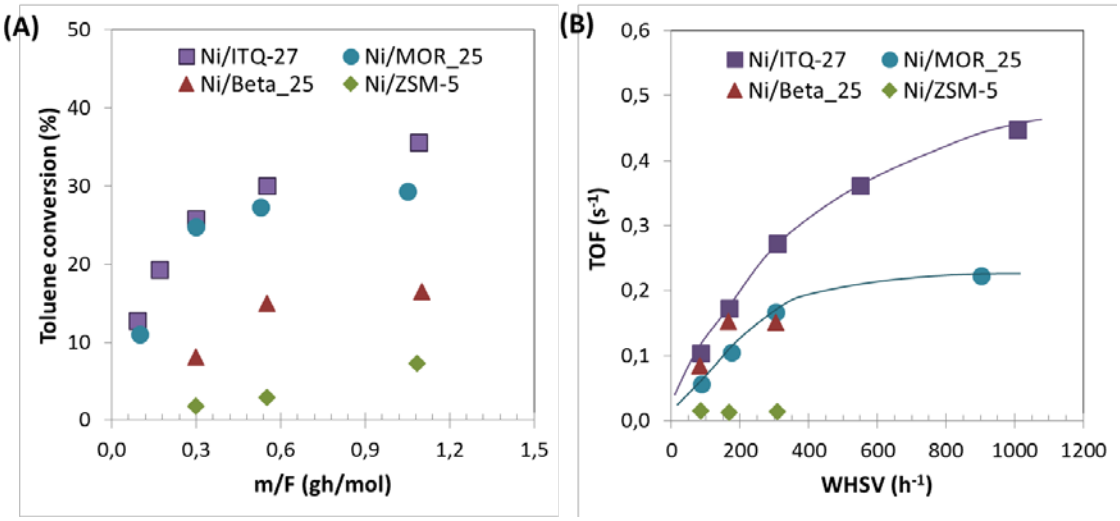

Figure 3: (A) Reaction mechanism for the acid catalyzed ethylbenzene isomerization reaction towards xylenes, and (B) Proposed ethylbenzene isomerization transition state mimic (TSM) as organic structure directing agent (OSDA)

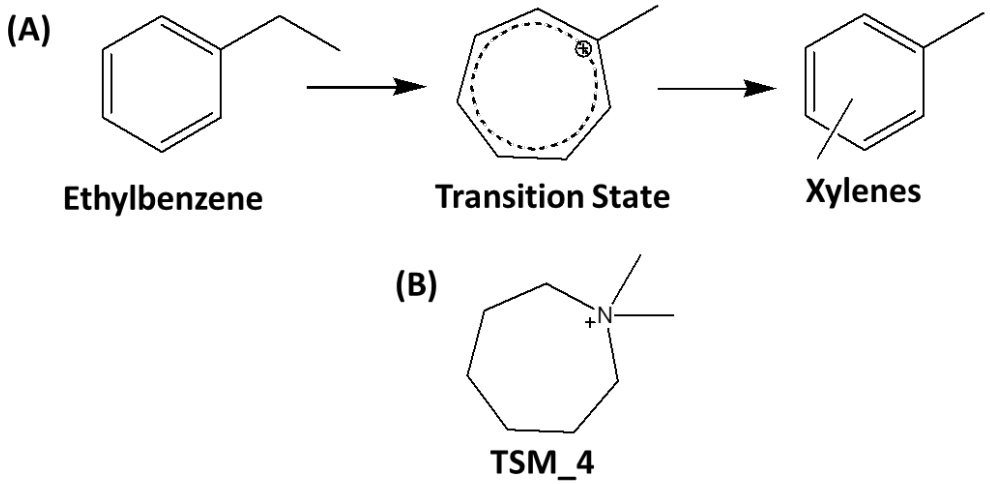

Figure 4: Selectivity to xylene isomers versus time-on-stream (TOS) for the ethylbenzene isomerization reaction using different zeolites

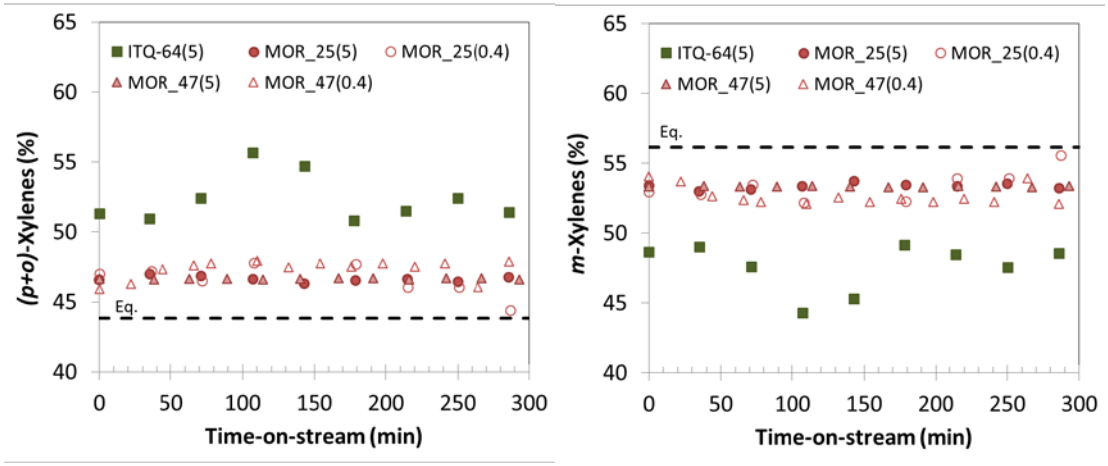

Figure 5: (A) Reaction mechanism for the *endo*-tricyclodecane isomerization, and (B) Proposed OSDAs as TSM for the *endo*-tricyclodecane isomerization

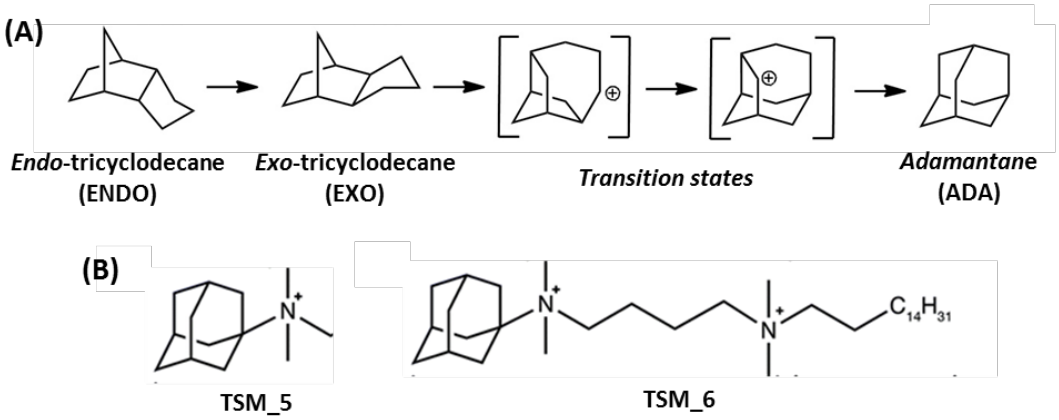

Table 1: Ethylbenzene conversion and product distribution achieved for the ethylbenzene isomerization using different zeolites (TOS = 30 min)

Catalyst	**ITQ-64**	**MOR_25 (Si/Al=22)**		**MOR_47 (Si/Al=47)**	
m_{cat} (g)	1.00	0.15	1.00	0.13	1.00
m/F (g·h/mol)	5.06	0.38	5.06	0.40	5.06
EB conversion (%)	26.4	33.4	79.6	25.4	71.1
Yield (wt.%)					
Light HC	14.0	14.2	37.6	7.4	30.0
Aromatic HC	12.4	19.2	42.0	18.0	41.0
Aromatic Select. (wt.%)					
Benzene	11.0	31.7	39.4	33.1	38.5
Toluene	2.8	4.3	19.7	2.4	15.1
Xylenes	63.3	28.6	17.4	19.9	17.2
Diethylbenzenes	9.1	25.4	6.9	38.4	14.1
Trimethilbenzenes	0.3	2.4	2.1	0.5	1.6
Other aromatics	6.4	5.9	11.2	4.5	10.3
C10+ aromatics	7.2	1.6	3.2	1.2	3.2

Table 2: Catalytic activity for the *endo*-tricyclodecane isomerization at 300ºC and 60 bar

Catalyst	Time (min)	TMN conversion (%)	Selectivity EXO (%)	Selectivity ADA (%)
USY (CBV-720)	75	55.0	32.4	11.2
	180	72.0	29.6	11.4
Beta (CP811)	180	56.9	14.8	4.6
MCM-22	180	37.8	13.3	30.2
MIT-1	180	50.8	16.8	33.4

References:

1. W. Vermeiren, J. P. Gilson, *Top. Catal.* **52**, 1131-1161 (2009).
2. M. J. Climent, A. Corma, S. Iborra, *Chem. Rev.* **111**, 1072-1133 (2011).
3. D. E. De Vos, P. A. Jacobs, *Micropor. Mesopor. Mater.* **82**, 293-304 (2005).
4. P. A. Jacobs, M. Dusselier, B. F. Sels, *Angew. Chem., Int. Ed.* **53**, 8621-8626 (2014).
5. P. Y. Dapsens, C. Mondelli, J. Perez-Ramirez, *ACS Catal.* **2**, 1487-1499 (2012).
6. M. E. Davis, *Chem. Mater.* **26**, 239-245 (2014).
7. M. Moliner, F. Rey, A. Corma, *Angew. Chem., Int. Ed.* **52**, 13880-13889 (2013).
8. J. Heilmann, W. F. Maier, *Angew. Chem., Int. Ed.* **33**, 471-473 (1994).
9. G. Wulff, B. Heide, G. Helfmeier, *J. Am. Chem. Soc.* **108**, 1089-1091 (1986).
10. W. R. Ahmad, M. E. Davis, *Catal. Lett.* **40**, 109-114 (1996).
11. A. Katz, M. E. Davis, *Nature* **403**, 286-289 (2000).
12. J. E. Lofgreen, G. A. Ozin, *Chem. Soc. Rev.* **43**, 911-933 (2014).
13. T. C. Tsai, S. B. Liu, I. Wang, *Appl. Catal. A* **181**, 355-398 (1999).
14. J. Cejka, B. Wichterlova, *Catal. Rev.* **44**, 375-421 (2002).
15. Y. Xiong, P. G. Rodewald, C. D. Chang, *J. Am. Chem. Soc.* **117**, 9427-9431 (1995).
16. D. L. Dorset, G. J. Kennedy, K. G. Strohmaier, M. J. Diaz-Cabañas, F. C. Rey, A. , *J. Am. Chem. Soc.* **128**, 8862–8867 (2006).
17. X. Xiao, J. Butler, C. Comeaux, K. K., *U.S. Patent 20060211902, 2006*.
18. J. R. Butler, X. Xiao, R. Hall, *U.S. Patent 20080319243, 2008*.
19. F. Moreau *et al.*, *J. Catal.* **202**, 402-412 (2001).
20. L. D. Fernandes, J. L. F. Monteiro, E. F. Sousa-Aguiar, A. Martinez, A. Corma, *J. Catal.* **177**, 366-377 (1998).
21. H. Pines, T. W. Greenlee, *J. Org. Chem.* **26**, 1052-1057 (1961).
22. L. Schreyeck, P. Caullet, J. C. Mougenel, J. L. Guth, B. Marler, *Micropor. Mater.* **6**, 259-271 (1996).
23. T. Ikeda, S. Kayamori, F. Mizukami, *J. Mater. Chem.* **19**, 5518-5525 (2009).
24. R. Millini *et al.*, *Microporous Mesoporous Mater.* **74**, 59-71 (2004).
25. A. Burton, R. J. Accardi, R. F. Lobo, M. Falconi, M. W. Deem, *Chem. Mater.* **12**, 2936-2942 (2000).
26. D. L. Dorset, G. J. Kennedy, *J. Phys. Chem. B* **108**, 15216-15222 (2004).
27. L. M. Knight *et al.*, *Stud. Surf. Sci. Catal.* **170**, 338-340 (2007).
28. T. Ikeda, S. Kayamori, Y. Oumi, F. Mizukami, *J. Phys. Chem. C* **114**, 3466-3476 (2010).
29. J. Ruan *et al.*, *Chem. Mater.* **21**, 2904–2911 (2009).
30. K. H. Robschlager, E. G. Chrlstoffe, *Ind. Eng. Chem. Prod. Res. Dev.* **18**, 347-352 (1979).
31. *Advances in adamantane research and application, Ed. Q. A. Acton, ScholarlyEditions, Atlanta, 2013*.
32. B. J. Mair, M. Shamaiengar, N. C. Krouskop, F. D. Rossini, *Anal. Chem.* **31**, 2082-2083 (1959).
33. P. R. Schleyer, *J. Am. Chem. Soc.* **79**, 3292–3292 (1957).
34. E. M. Engler, M. Farcasiu, A. Sevin, J. M. Cense, P. V. R. Schleyer, *J. Am. Chem. Soc.* **95**, 5769-5771 (1973).
35. G. C. Lau, W. F. Maier, *Langmuir* **3**, 164-173 (1987).
36. K. Honna, M. Sugimoto, N. Shimizu, K. Kurisaki, *Chem. Lett.*, 315-318 (1986).
37. Z. Gao, H. B. Yang, *Chin. J. Chem.* **12**, 52-57 (1994).
38. M. Navrátilová, K. Sporka, *Appl. Catal. A* **203**, 127-132 (2000).
39. P. R. Schleyer, M. M. Donaldson, *J. Am. Chem. Soc.* **82**, 4645-4651 (1960).
40. S. I. Zones, *U.S. Patent 4544538, 1985*.
41. M. J. Diaz, M. A. Camblor, C. Corell, A. Corma, *US Patent, 6077498, 2000*.

42. A. Corma, V. Fornes, S. B. Pergher, T. L. M. Maesen, J. G. Buglass, *Nature* **396**, 353-356 (1998).
43. H. Y. Luo, V. K. Michaelis, S. Hodges, R. G. Griffin, Y. Roman-Leshkov, *Chem. Sci.* **6**, 6320-6324 (2015).
44. V. J. Margarit, M. E. Martínez-Armero, M. T. Navarro, C. Martínez, A. Corma, *Angew. Chem., Int. Ed.* **54**, 13724 -13728 (2015).